Exciton broadening and spin dynamics in III-V/II-VI:Mn heterovalent double quantum wells

A. A. Toropov, Ya. V. Terent'ev, P. S. Kop'ev, and S. V. Ivanov
Ioffe Physico-Technical Institute, Russian Academy of Sciences, Politekhnicheskaya 26, 194021 St. Petersburg, Russia

T. Koyama, K. Nishibayashi, A. Murayama, and Y. Oka
Institute of Multidisciplinary Research for Advanced Materials, Tohoku University, Sendai 9808577, Japan

A. Golnik and J. A. Gaj
Institute of Experimental Physics, Warsaw University, 00-681 Warsaw, Poland
(Received 3 March 2008; published 13 June 2008)

We report on the optical studies of exciton broadening mechanisms and exciton spin dynamics in diluted magnetic semiconductor GaAs/AlGaAs/ZnSe/ZnCdMnSe heterovalent double quantum wells (QWs) grown by molecular-beam epitaxy. The heterovalent interface manifests itself in the fluctuations of the interface dipole moment and, hence, in an enhanced inhomogeneous broadening of the excitonic emission, as well as in generation of type-II localized excitons. Microphotoluminescence measurements indicate that these fluctuations occur on the scale less than 1 μm. The rise curves of circular polarization of the excitonic emission are measured in an external magnetic field. The kinetics of the exciton spin polarization is strongly affected by the strength of electronic coupling between the GaAs/AlGaAs and ZnSe/ZnCdMnSe QWs, as well as by the factor of the exciton inhomogeneous broadening. Depending on these parameters, the relaxation time of the net spin polarization in the structures varies from the values shorter than 20 ps up to ~9 ns.

DOI: 10.1103/PhysRevB.77.235310 PACS number(s): 78.67.Pt, 85.75.Mm, 75.70.Cn

I. INTRODUCTION

Electronic properties of heterovalent structures involving semiconductor compounds of different chemical groups have long been of interest. The early studies were focused on theoretical calculations of the stability of different atomic reconstructions at heterovalent interfaces[1,2] and elucidation of the electrical dipole effects on the band-edge discontinuities.[3,4] Later the process of the formation of heterovalent interfaces was studied in detail for the growth of device heterostructures on lattice-matched substrates of a different chemical group. The most known attempt of this kind is the utilization of GaAs substrates for the subsequent growth of blue-green light-emitting devices based on ZnSe.[5] The diffusive transport of spin-polarized electrons through the III-V/II-VI heterovalent interface was observed in Ga(In)As/(Al)GaAs light-emitting diodes with a deposited layer of a II-VI diluted magnetic semiconductor (DMS).[6] Furthermore, a huge valence-band offset (VBO) at an InAs/CdSe heterovalent interface was used as a key factor to reduce hole leakage in midinfrared optoelectronic devices based on InAs.[7] All these applications relied on flexible engineering of band discontinuities at the heterovalent junctions and efficient transport of carriers achieved in the state-of-the-art heterovalent structures.

Recently, heterovalent double quantum wells (QWs) have been designed and fabricated, where a III-V QW (GaAs/AlGaAs) and a II-VI DMS QW (ZnCdMnSe/ZnSe) are electronically coupled through a thin barrier incorporating an AlGaAs/ZnSe heterovalent interface.[8,9] These structures were intended to combine advantages of III-V nonmagnetic semiconductors and II-VI DMS in a monolithic device aimed for spintronic applications. In particular, it was expected to obtain strong spin polarization of carriers in a weak external magnetic field, which is typical for II-VI DMS, in a nonmagnetic GaAs QW demonstrating typically high carrier mobility and long spin relaxation time. In agreement with the design of the structure, magnetophotoluminescence (magneto-PL) measurements demonstrated strong renormalization of the excitonic magnetic g factor, induced by electronic coupling between the nonmagnetic GaAs/AlGaAs QW and the DMS ZnCdMnSe/ZnSe QW.[8] Simultaneously, the observed linewidth of excitonic emission in the heterovalent double QWs (DQWs) was two to three times larger than the energy corresponding to a single-monolayer fluctuation of the GaAs QW thickness. This enhanced inhomogeneous broadening implies the emergence of a specific fluctuating localization potential induced by chemical disordering of the heterovalent interface.[9]

In this paper, we study the effect of a heterovalent interface on the exciton localization potential in GaAs/AlGaAs/ZnSe/ZnCdMnSe DQWs using a micro-PL setup with the spatial resolution better than 1 μm. Furthermore, a time-resolved PL spectroscopy in an external magnetic field is applied to elucidate the consequences of the exciton inhomogeneous broadening on the recombination and spin dynamics of carriers in these structures. The paper is organized as follows. Section II describes the samples and experimental techniques. Section III presents the results of micro-PL experiments and time-resolved magneto-PL measurements. In Sec. IV we discuss the issue of the exciton inhomogeneous broadening as well as the peculiarities of recombination and spin dynamics of excitons in the DQW structures. Finally, Sec. V concludes the paper.

II. SAMPLES AND EXPERIMENTAL TECHNIQUES

We performed comparative studies of two samples with a GaAs/AlGaAs/ZnSe/ZnCdMnSe DQW, fabricated by

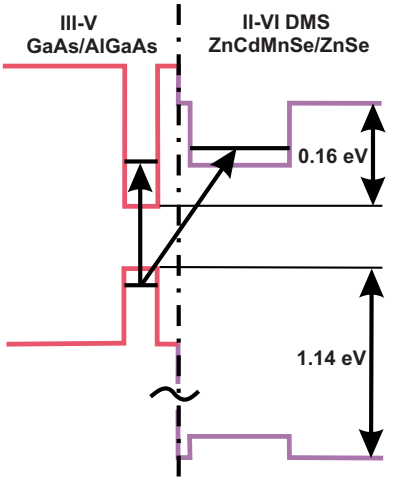

FIG. 1. (Color online) Schematic representation of band line-ups in the AlGaAs/GaAs/ZnSe/ZnCdMnSe DQW structures. The growth direction is from left to right.

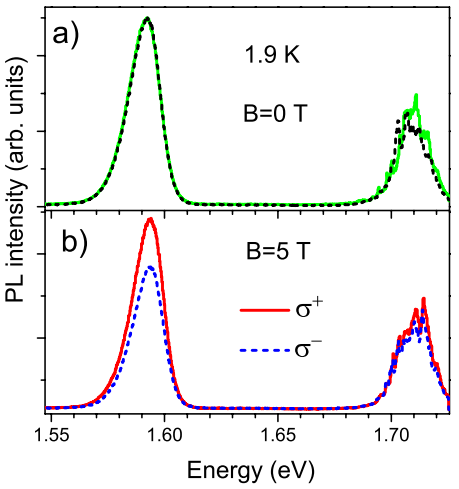

FIG. 2. (Color online) (a) Micro-PL spectra measured in the non-resonant DQW sample at two typical points at the magnetic field $B=0$ T. The points correspond to nearly the same intensity of the illumination. The spectra are normalized to the intensity of the low-energy peak. (b) Circularly polarized (σ^+ and σ^-) micro-PL spectra measured at a certain point of the nonresonant DQW sample at the magnetic field $B=5$ T.

molecular-beam epitaxy. The growth of the AlGaAs/ZnSe heterovalent interface in both structures was optimized in the attempt to produce a neutral compensated interface with a vanishing average dipole moment along the growth direction. Therefore the conduction-band offset (CBO) and VBO are expected to approach the values of chemical band offsets. More data on the growth procedure and design of the samples can be found elsewhere.[8,9] In both structures the width of the ZnCdMnSe QW is 9 nm and the thickness of the combined AlGaAs/ZnSe barrier between the QWs amounts to 3.2 nm. The samples differ in the width of the GaAs QW. The structure with the 3.2 nm thick GaAs QW can be considered as resonant since the estimated average detuning of the ground electron levels in the two QWs (~10 meV) is comparable with the expected level anticrossing gap. The other structure contains 5 nm wide GaAs QW and the gap between the two electron levels amounts to 30 meV, so that the level confined in the GaAs QW is the lowest one. In the following discussion, we mention this sample as "nonresonant." The band line-up of the structures is shown schematically in Fig. 1. One should note that the nonresonant sample contains additionally a 2.8 nm wide GaAs single QW placed 15 nm apart from the heterovalent interface within bulk AlGaAs.

For micro-PL measurements, the samples were mounted on a specially designed confocal microscope (see Ref. 10), which was then immersed in superfluid helium in the cryostat with a superconducting magnet. The magnetic field was applied in the Faraday configuration. Photoluminescence mapping was accomplished using a plane-parallel fused-silica plate placed between the microscope and the first lens of the optical system. The plate was rotated around two perpendicular axes by step motors similarly as in the system described in Ref. 11. The typical area of scans was 20 $\times 20$ μm^2. Photoluminescence spectra were taken by a charge-coupled device camera fixed at the spectrograph exit. A 532 nm *cw* solid-state laser was used for excitation. The maps were obtained by sweeping the excitation spot (diameter no more than 1 μm) with a step of 1 μm. The spectra were fit with Gaussian lines, allowing us to construct the maps of various parameters. The illumination of the map area was inhomogeneous. This allowed one to measure the correlation between line intensity and line position, resulting from varying excitation density. The excitation power before the microscope was 5 μW. This sets the upper limit for the power density assuming the spot diameter of 1 μm since we estimate that less then half of the power reaches the excitation spot. However the spot size might be as well two times smaller and the observed size of luminescence spot can be due to diffusion of excited carriers for the overbarrier excitation.

The PL spectra with time resolution were measured using a double-frequency emission of a mode-locked Ti:sapphire laser with the 76 MHz repetition frequency and subpicosecond pulse width. The diameter of the spot on the sample was about 0.3 mm. The polarization of the laser emission was linear. A Hamamatsu syncroscan streak camera was used for detection. The time resolution of the setup was estimated as 15 ps. An external magnetic field was applied in Faraday geometry using a split-coil superconducting magnet.

III. EXPERIMENTAL RESULTS

A. Microphotoluminescence spectroscopy

Figure 2 shows typical micro-PL spectra measured in the nonresonant sample at zero magnetic field [Fig. 2(a)] and at $B=5$ T [Fig. 2(b)]. Besides the emission lines of a GaAs substrate and buffer layer (not shown in Fig. 2), there are two peaks in the spectra. The PL peak at 1.59 eV is attributed to the emission of the GaAs/AlGaAs/ZnSe/ZnCdMnSe DQW and the peak at 1.71 eV is ascribed to the emission of the reference GaAs/AlGaAs single QW placed 15 nm apart from the heterovalent interface. The latter line displays a fine

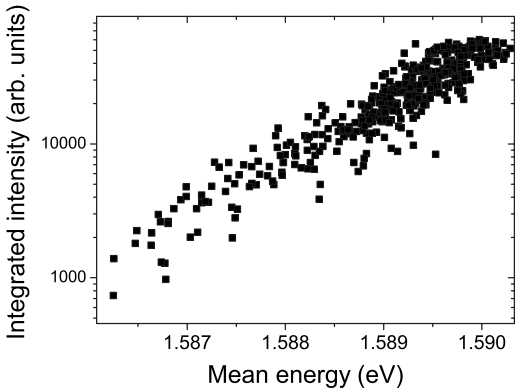

FIG. 3. The diagram of correlation between the integrated intensity and mean energy for the line at 1.59 eV in the nonresonant DQW sample. The variation of the PL intensity is due to the inhomogeneous illumination of the map area.

structure varying across the map. This observation is consistent with the previously reported spatially resolved PL spectra of thin GaAs/AlGaAs QWs, demonstrating narrow lines of single excitons localized by interface fluctuations.[12] In contrast to that, the line at 1.59 eV is fairly smooth and well reproducible across the map in the areas with close intensity of the illumination. No fine structure can be observed within this line. Application of the magnetic field practically does not influence the spectrum of the reference QW that is consistent with the negligibly small magnetic g factor expected for excitons in the GaAs/AlGaAs single QW. The emission of the DQW is σ^+ polarized with a polarization degree of $\sim$16%. The diagram in Fig. 3 shows the correlation between the line intensity and mean energy for the line at 1.59 eV in the nonresonant DQW sample. The diagram is obtained by fitting the spectrum at different points of the map, whereas the variation of the PL intensity is due to the inhomogeneous illumination of the map area. One can see in Fig. 3 that the increase in the excitation power density results in a small shift of the line toward higher energy.

Figure 4(a) shows the micro-PL spectra measured at different points across the map in the resonant sample at zero magnetic field. There is a line at 1.64 eV, attributed to the emission of the DQW. Like in the nonresonant DQW, no narrow peaks of single excitons can be typically observed within this line. In contrast to the nonresonant sample, the shape of the spectrum varies across the map. For most of the measurement points within the tested area (20×20 μm^2), the variation is rather weak and smooth, whereas at a certain area (3×3 μm^2), the spectrum shape is quite different—the lower-energy tail of the smooth PL line is superposed by narrower peaks. Note that these peaks can hardly be considered as lines of single localized excitons since their spectral width (2–10 meV) is still quite large. Figure 5(a) illustrates the correlation between the line intensity and mean energy for the resonant sample. One can see that the shift toward higher energies with the increase in the excitation power is in this sample stronger than in the nonresonant one.

The micro-PL spectra measured in the resonant sample at the magnetic field B=5 T for the two circular polarizations are shown in Fig. 4(b), both for a typical and a nontypical

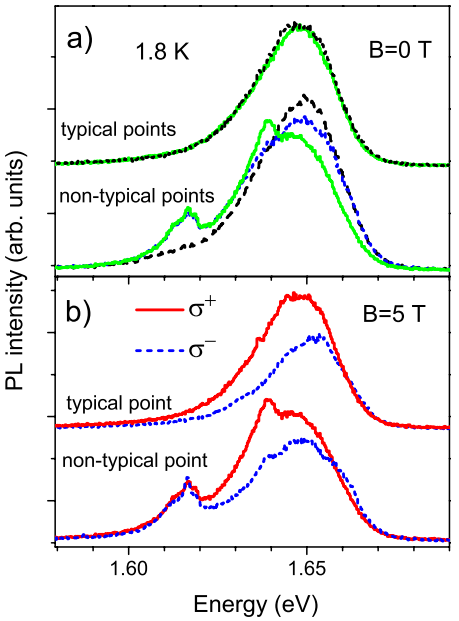

FIG. 4. (Color online) (a) Micro-PL spectra measured in the resonant DQW sample at two typical points and three non-typical points at zero magnetic field. The nontypical points are separated from each other by 1 μm. All points correspond to nearly the same intensity of the illumination. (b) Circularly polarized (σ^+ and σ^-) micro-PL spectra measured at a typical and a nontypical point of the resonant DQW sample at the magnetic field $B=5$ T. In both figures, a vertical offset between the spectra measured at the typical and nontypical points is introduced for clarity.

point. The magnetic field results in a variation of the line shape and strong σ^+ polarization. On the average, the σ^+-polarized spectrum is shifted toward lower energy as compared with the σ^--polarized one. The narrow lines observed at nontypical points do not show any specific splitting in the magnetic field. The degree of σ^+ circular polarization within these peaks differs (is typically greater) from the polarization detected at the same energy within the smooth line measured at typical points. Figure 5(b) shows the diagram of the correlation between the line intensity and the polarization degree at 5 T. The local values of the polarization degree

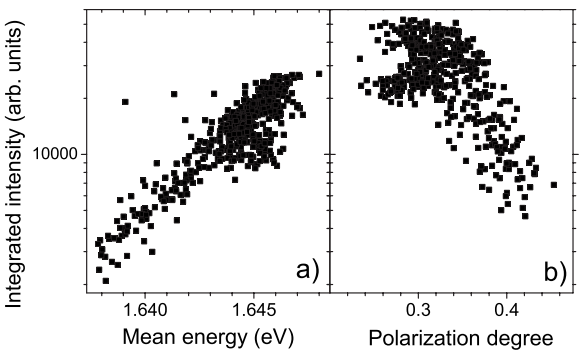

FIG. 5. The diagram of correlation between the peak integrated intensity and mean energy at $B=0$ T (a) and the peak intensity and σ^+ circular polarization at $B=5$ T (b) for the line at 1.64 eV in the resonant DQW sample. The variation of the PL intensity is due to the inhomogeneous illumination of the map area.

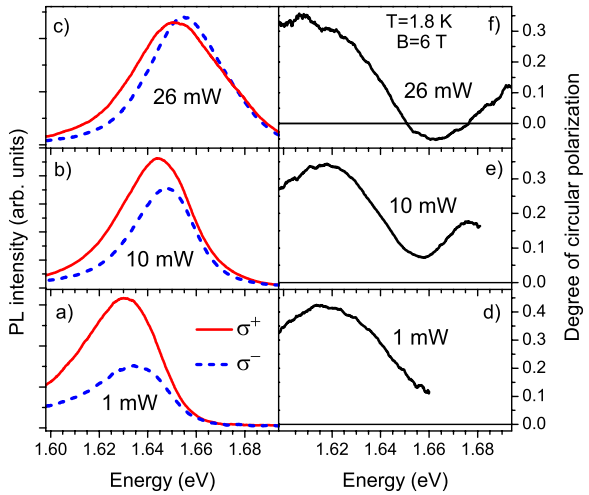

FIG. 6. (Color online) [(a)–(c)] Spatially averaged circularly polarized PL spectra measured in the resonant DQW sample at $B=6$ T and different average excitation powers. [(d)–(f)] Respective spectra of the degree of σ^+ circular polarization.

differ drastically across the map area (from 0.23 to 0.45). Furthermore, certain correlation is well visible—the decrease in the excitation power results in an average increase in the polarization degree.

To avoid the complication caused by the lateral fluctuations of the polarization degree, we have measured the spatially averaged power-dependent PL spectra in a conventional geometry with the excitation spot size of ~0.3 mm. The time-integrated PL was measured in the resonant DQW sample using a double-frequency emission of a mode-locked Ti:sapphire laser as an excitation source. The spectra obtained at the magnetic field of 6 T and different excitation powers are shown in Figs. 6(a)–6(c). Both the peak position and the polarization degree depend on the excitation power. At the lowest average excitation power, the polarization degree is positive everywhere within the PL line and the maximum value exceeds 40% [see Figs. 6(d)–6(f)]. The increase in the excitation power leads to the development of the high-energy tail of the line, accompanied by the shift of the line maximum. Simultaneously, the polarization degree integrated over the spectrum decreases, mostly due to the smaller PL polarization at the higher-energy part of the line, revealed at the enhanced excitation. At the strongest excitation (26 mW), the polarization changes the sign from positive to negative in a narrow spectral region around 1.66 eV.

B. Time-resolved magnetophotoluminescence spectroscopy

Both nonresonant and resonant DQW samples demonstrate a rather complicated transient behavior of the emission after the excitation pulse.[9] In particular, the PL decay curves cannot be fitted within a single-exponential decay model at an arbitrary detection energy within the PL line. In the nonresonant sample, the two-exponential decay fit looks, however, quite reasonable practically everywhere within the PL contour. In this model, the decay curve is fitted as a sum of two decaying exponents,

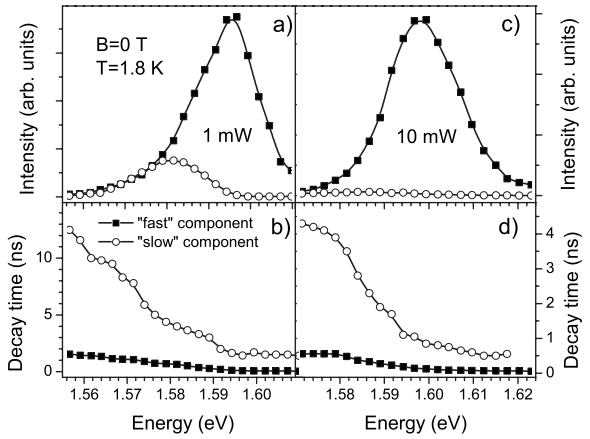

FIG. 7. [(a) and (c)] Relative intensities and [(b) and (d)] decay time constants of the slow (open circles) and fast (filled squares) components as obtained from a two-exponential decay fitting procedure of time-resolved PL spectra in the nonresonant sample (PL line at 1.59 eV). Magnetic field is 0 T, the excitation power is either [(a) and (b)] 1 mW or [(c) and (d)] 10 mW. The solid lines are plotted only to guide the eye.

$$I_{\mathrm{PL}}(t) = I_f e^{(-t\backslash\tau_f)} + I_s e^{(-t\backslash\tau_s)}, \tag{1}$$

Here τ_f and τ_s represent "fast" and "slow" decay constants and I_f and I_s are relative intensities of the two components. Figure 7 illustrates spectral dependencies of τ_f, τ_s, I_f, and I_s, as obtained in the nonresonant sample from the two-exponential fitting model for two excitation powers (1 and 10 mW). The "fast" component dominates for both values of the excitation power. The increase in the power is accompanied by a drastic saturation of the "slow" component so that at 10 mW its relative intensity is almost negligible. The enhancement of the excitation power affects also both decay constants; at any particular detection energy, their values decrease.

Figures 8(a) and 8(b) illustrate the effect of the magnetic field on the transient dynamics of circularly polarized PL in the nonresonant DQW. The degree of circular polarization strongly depends on the time delay. Immediately after excitation the polarization degree is close to zero. Subsequently the degree of σ^+ circular polarization increases, following the relaxation of net spin in the system. In order to fit the transient, we use rate-equation analysis to describe the dynamics of the densities of excitons, whose degeneracy is lifted by the external magnetic field. In this fitting procedure, we imply the existence of two types of excitons with different both radiative and spin lifetimes. This assumption is in agreement with the separation of the PL line at zero magnetic field into the fast and slow components, as shown in Fig. 7.

Only $\langle -1/2|3/2\rangle$ and $\langle 1/2|-3/2\rangle$ optically active ("bright") exciton populations can give rise to emission detected in the PL measurements. The exciton spin relaxation between the optically allowed states can occur in a direct single-step process driven by the electron-hole exchange interaction. In addition, the electron and the hole within an exciton can flip its spin separately. This leads to a transition between an optically allowed and forbidden ("dark") states ($\langle -1/2|-3/2\rangle$ and $\langle 1/2|3/2\rangle$ excitons).[13,14] Two such suc-

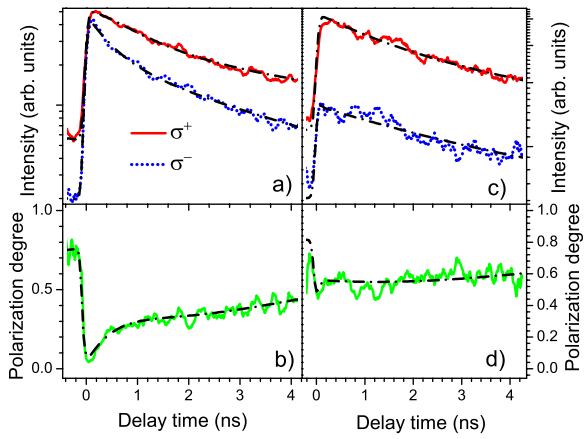

FIG. 8. (Color online) Temporal evolution of [(a) and (c)] circularly polarized PL and [(b) and (d)] the respective polarization degree detected either in the nonresonant sample ([(a) and (b)] detection energy of 1.57 eV] or in the resonant sample ([(c) and (d) detection energy of 1.62 eV] at the magnetic field $B=6$ T and the excitation power 1 mW. The theoretical fits to the experimental data are shown by the dash-dotted lines. Note different vertical scales in (a) and (c).

cessive transitions, one involving a hole and the other involving an electron, are necessary to go between "bright" exciton states. The relative contributions of the two mechanisms of spin relaxation in DQWs can depend on many factors, such as the electron-hole overlap integral, the spin scattering by magnetic ions, and the details of the exciton localization potential.

Due to this complexity, comprehensive description of the spin relaxation of bright excitons requires allowance for the dynamics of the population of dark excitons. In order to keep a reasonable number of fitting parameters, we neglect in our analysis the transitions to the dark excitonic states and, hence, characterize the relaxation process by a single spin scattering constant. While this simplified model is inadequate to describe the detailed dynamics of the exciton system, it nevertheless provides an estimate of the recombination and spin-relaxation rates. For simplicity, we also neglect the impact of nonradiative recombination.

Under these assumptions, the rate equations are the following:

$$\frac{d}{dt}\begin{pmatrix} n^+_{1,2} \\ n^-_{1,2} \end{pmatrix} = \begin{pmatrix} N^+_{1,2} e^{-t^2/\Delta t^2} \\ N^-_{1,2} e^{-t^2/\Delta t^2} \end{pmatrix} + \begin{pmatrix} -\frac{1}{\tau^r_{1,2}} - \frac{1}{\tau^s_{1,2}} & \frac{1}{\tau^s_{1,2}} e^{-\Delta E_{1,2}/k_B T} \\ \frac{1}{\tau^s_{1,2}} & -\frac{1}{\tau^r_{1,2}} - \frac{1}{\tau^s_{1,2}} e^{-\Delta E_{1,2}/k_B T} \end{pmatrix} \times \begin{pmatrix} n^+_{1,2} \\ n^-_{1,2} \end{pmatrix}. \quad (2)$$

Here n^+_i and n^-_i are the density of spins in the upper- and lower-energy spin states, respectively. The index $i=1$ denotes the quantities corresponding to the "fast" component of the exciton population, while $i=2$ corresponds to those of the "slow" component. τ^r_i is the recombination lifetime of the excitons, and τ^s_i is the spin-scattering time between the two spin states. The Boltzmann factor $\exp(-\Delta E_i/k_B T)$ describes thermal activation of the excitons, ΔE_i denotes the spin splitting energy for the ith population of the excitons, and T is the electronic temperature. For simplicity we assume that the spin splitting of excitonic levels is much smaller than the exciton inhomogeneous broadening (20–40 meV). This is reliably justified for the type I excitons, when both electron and heavy hole are confined in the nonmagnetic GaAs/AlGaAs QW and the spin splitting is negligible. The spin splitting of the mixed excitonic states, when the electron penetrates into the DMS ZnCdMnSe/ZnSe QW, can be estimated as 8–9 meV (see discussion in Sec. IV). The generation rate of excitons in each state from the laser pulse of width Δt is represented by the first term on the right side of the equation. In the fitting procedure we assume that $N^+_i = N^-_i$, which is relevant to the linear polarization of the laser pulse. The ratio $\frac{N^\pm_1}{N^\pm_2}$ was used as a fitting parameter defining the relative contributions from the two populations of the excitons. The fits to the measured decay curves of the σ^+- and σ^--polarized emission are calculated as

$$I_{\sigma^+,\sigma^-}(t) = I_0 + \sum_i \frac{n^{\mp}_i(t)}{\tau^r_i}, \quad (3)$$

where I_0 is the constant fitting parameter that takes account of a certain background emerging in the experimental curves. For the comparison with the experimental data, the calculated decay curves were convoluted with the measured response function of the detection system. Since the PL signal does not decay completely within the period between the laser pulses (~12 ns), in the calculated curves we added the contributions from sequential pulses, until the shape of the curves becomes independent of the number of the periods taken into account.

The best fits to the decay curves measured in the nonresonant sample at a certain detection energy (1.57 eV) at the magnetic field 6 T are shown in Fig. 8(a) together with the experimental data. Figure 8(b) shows the respective transients of the degree of σ^+ polarization. To obtain these perfect fits, the following parameters were substituted: $\tau^r_1 = 850$ ps, $\tau^r_2 = 5.2$ ns, $\tau^s_1 = 900$ ps, and $\tau^s_2 = 8.6$ ns. It was also assumed that $\Delta E_1 = 2k_B T$ and $\Delta E_2 \gg k_B T$. For the low temperatures used it corresponds to the ΔE_1 values less than 0.5 meV and ΔE_2 values higher than at least 1 meV.

The emission dynamics in the resonant DQW at zero magnetic field is roughly similar to that in the nonresonant one.[9] However, the fraction of the slowly decaying component in this sample is much larger. In the limit of weak excitation the slow component dominates. An increase in the excitation power results in an easy saturation of the slowly decaying emission. As a result, the fast component is revealed at the high-energy wing of the emission line. In contrast to the nonresonant DQW the slow component does not saturate completely at higher excitation powers, remaining dominant within the lower-energy tail of the PL line. In the time-integrated spectra the effect of the selective saturation

of the slow component of the emission manifests itself as the blueshift of the line maximum (see Fig. 6).

The spin dynamics of excitons in the external magnetic field in this sample is, however, qualitatively different [see Figs. 8(c) and 8(d)]. A noticeable spin polarization (~50%) is established instantly after the excitation pulse and then is almost constant within a few nanoseconds. A reasonable fitting of these curves could be made only under the assumption that for a certain fraction of the exciton density the spin-relaxation rate is faster than the time resolution of the setup. On the other hand, the relatively low degree of polarization implies the existence of excitons with a spin-relaxation rate in the range of a few nanoseconds. The dash-dotted lines in Figs. 8(c) and 8(d) show the best fit to the experimental data, obtained using the same theoretical model as we used for describing the exciton dynamics in the nonresonant sample. We also assume that $\Delta E_{1,2} \gg k_B T$, which is consistent with the enhanced penetration of the electron wave function into the DMS QW in the resonant structure. The following parameters were used to obtain this fit: $\tau_1^r = 2$ ns, $\tau_2^r = 9$ ns, $\tau_1^s < 20$ ps, and $\tau_2^s = 8$ ns. It is interesting to note that the spin-relaxation rate obtained for the slow component of the excitonic emission is practically the same for the resonant and nonresonant samples.

IV. DISCUSSION

The inhomogeneous broadening of excitons in conventional semiconductor QWs emerges due to fluctuations of the QW width and fluctuations of the composition of the involved solid alloys. An additional broadening can take place in the heterovalent QWs with polar heterovalent interfaces due to fluctuations of the electrical dipole moment near the interface due to the unavoidable presence of donorlike and acceptorlike charged interface bonds.[3] It is currently well understood that thermodynamics favors the formation of a chemically mixed interface, while the structure of a homogeneous abrupt interface is unstable.[2] For the GaAs/ZnSe interface it was predicted that the most probable interface structure is a statistical mixture of lateral areas, representing either one mixed layer of cations (Ga-Zn) or one mixed layer of anions (As-Se). Within each microscopic area, a compensated interface is favored, with equal number of donor and acceptor bonds. The mixed single-layer structure is energetically degenerate with respect to polarity and, hence, the formation probability does not depend on whether the mixed interface layer consists of anions or cations and builds up a positive or negative dipole moment.[2] Thus, under growth conditions close to equilibrium one can expect that both polarities occur in a ratio of about 1:1 and the average dipole moment of the interface nearly vanishes. Nevertheless locally the dipole moment is large so that essential fluctuations of the interface dipole moment are expected on the microscopic scale. Currently there is no theory predicting the characteristic size of these fluctuations.

Molecular beam epitaxy is a strongly nonequilibrium growth process. Following the results of Nicolini *et al.*,[4] we ensured the growth conditions typical for realization of chemical band offsets at the interface, i.e., of nearly vanishing average dipole moment along the growth axis. Nevertheless, due to the nonequilibrium nature of the formation process, on the microscopic level the structure can differ from the theoretical prediction made for equilibrium conditions. For example, the two-mixed-layer formation is quite possible with a more complicated distribution of cations and anions of different kinds within these layers. In any case, a strongly inhomogeneous electric field fluctuating on the microscopic scale is expected to emerge in the very vicinity of the interface. Let us now consider the experimental results presented in Sec. III, bearing in mind possible influence of the interface electric fields on exciton properties.

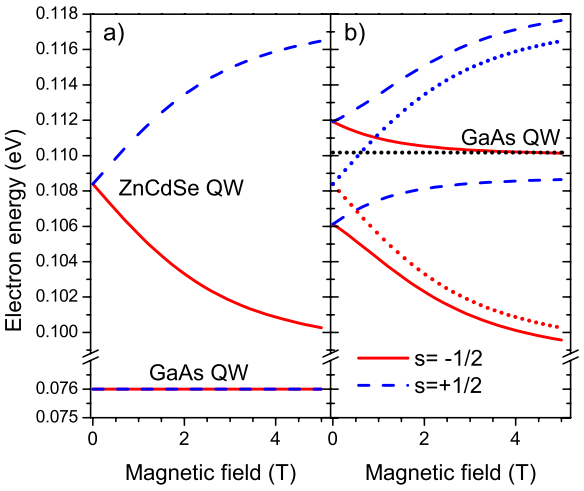

FIG. 9. (Color online) Electron levels versus magnetic field in the (a) nonresonant DQW and (b) resonant DQW. The dotted curves in (b) represent the levels in an isolated GaAs/AlGaAs QW and ZnCdMnSe/ZnSe QW. The mixed levels in the coupled QWs are plotted by solid lines (electron spin $s=-1/2$) and dashed lines (electron spin $s=+1/2$).

The heavy hole in the excitons is always strongly confined in the nonmagnetic GaAs/AlGaAs QW (see Fig. 1). Due to the small g factor, the hole energy level is practically independent of the magnetic field. Therefore the exciton energies reflect mainly the effect of giant Zeeman splitting of electron levels penetrating into the DMS region, being only slightly corrected due to the magnetic-field dependence of the exciton binding energies.[8] Figure 9 demonstrates calculated dependencies of the electron energy levels versus magnetic field in the nonresonant DQW [Fig. 9(a)] and resonant DQW [Fig. 9(b)]. In this calculation we neglect both diamagnetic shift of the levels and their Zeeman splitting due to the intrinsic g factor since both effects are much weaker than the effect of giant Zeeman splitting in the DMS ZnCdMnSe layer. In the nonresonant DQW, the energy gap between the single-QW levels at zero magnetic field (~30 meV) is large enough and the levels are practically decoupled at any magnetic field. Therefore, one can expect the spatially direct exciton in the DQW to behave like an exciton in a conventional GaAs/AlGaAs single QW. Indeed, the kinetics of the dominant fast contribution to the PL line (see Fig. 7) is typical to the kinetics of localized excitons in a single QW; like there, the exciton decay time constant varies from a few tens of picoseconds at the high-energy part of the line to a few hun-

dreds of picoseconds at the low-energy tail. The spin-relaxation rate obtained for the fast component of the excitonic emission also looks reasonably for localized excitons in the nonresonant DQW, where the electron wave function only weakly penetrates into the DMS QW. As shown in Fig. 7, the main difference from the kinetics of a single-QW exciton is the emergence of the slow component, where the decay time constant is in the nanosecond range.

To explain the long PL lifetime, one should assume that the overlap of the electron and hole wave functions within the exciton is relatively weak. There are two possibilities to spatially separate the electron and hole in the considered DQW structure. First, the fluctuations of either the QW width and composition of the solid alloy, or the fluctuations of the electric field near the heterovalent interface can result in the local reduction of the energy of electrons confined in the ZnCdMnSe QW. When this electron level shifts below the electron level in the GaAs QW, the lowest-energy exciton becomes a type-II exciton, where the hole is confined within the GaAs QW and the electron is located within the ZnCdMnSe QW. Their overlap is reduced and the exciton radiative lifetime is enhanced. Another possibility takes place when both electron and hole are confined within the GaAs QW, but their overlap is reduced due to the action of the local electric fields induced by the interface.

It is possible to distinguish between the two mechanisms, studying the effect of the magnetic field on the circular polarization of the excitonic emission. At a certain external magnetic field, the degree of circular polarization depends on the electron and hole g factor and the rate of spin relaxation. In a conventional 5 nm thick GaAs/AlGaAs QW the electron g factor is practically equal to zero and the heavy-hole g factor is also quite small (see, e.g., Ref. 15). Therefore the exciton spin splitting at reasonably small magnetic fields ($\mathbf{B} \lesssim 5$ T) is smaller than the thermal energy $k_B T$ and the polarization degree is low. The application of the electric field does not change noticeably the value of g factors but reduces the rate of spin relaxation via the decrease in the electron-hole exchange interaction.[14,16] Under the conditions of linearly polarized excitation, the decrease in the spin-relaxation rate should further reduce the degree of the circular polarization. The lowest allowed spin-split exciton in the 5 nm thick GaAs/AlGaAs QW is the σ^- polarized $\langle 1/2 | -3/2 \rangle$ exciton.[15] As a result, the emission of excitons in the GaAs/AlGaAs QW exposed to the electric field should be weakly σ^- polarized. This contradicts the observation of strong (70%–80%) σ^+ polarization of the emission at the delay time ~ 12 ns [see Figs. 8(a) and 8(b)]. Hence we assume that the slow component owes mainly to the emergence of the type-II excitons with the electron wave function strongly confined in the DMS QW. This interpretation implies that the respective electron localization energy in the ZnCdMnSe QW is in the range of 50–60 meV [see Figs. 7(a) and 9(a)]. Bearing in mind that the local variation of CBO at the GaAs/ZnSe interface, induced by the fluctuations of the interface dipole moment, can be as large as 0.6 eV,[2] this value of the localization energy looks quite possible.

In the resonant DQW, the magnetic field lifts off the spin degeneracy for all four electron levels [see Fig. 9(b)]. This is the result of resonant electronic coupling between the nonmagnetic and DMS QWs. The spin splitting of the ground electron state and, hence, of the ground excitonic state is in the range of a few millielectronvolts at 5–6 T. In the limit of high magnetic fields the lowest $\langle -1/2 | 3/2 \rangle$ σ^+-polarized exciton in the coupled QWs approaches the type-II exciton (with the electron essentially confined within the ZnCdMnSe QW), while the $\langle 1/2 | -3/2 \rangle$ σ^--polarized excitonic state approaches the type-I exciton (with the electron confined within the GaAs QW). One can expect that the emission of the ground-state σ^+-polarized excitons should dominate at relatively weak excitation, whereas stronger excitation saturates the long-living type-II excitonic states and reveals the emission of σ^- polarized type-I excitons with larger oscillator strength and shorter radiative lifetime. This is the behavior demonstrated in Fig. 6. Note that the effect of the saturation of circular polarization, observed both in resonant and nonresonant structures, should be typical for any DMS DQW of similar design, irrespectively of its heterovalent or isovalent structure. The effect of the heterovalent interface in this case is quantitative rather than qualitative since it leads mainly to some additional inhomogeneous broadening induced by the fluctuations of the electrical dipole moments near the interface. Nevertheless, the emergence of the long-living σ^+-polarized excitons in the nonresonant DQW with the ~ 30 meV gap between the single-QW electron levels can hardly be explained considering only conventional broadening mechanisms determined by the fluctuations of the QW width and composition. We believe that the fluctuations of the interface dipole moment and resulting local electric fields are responsible for the emergence of the type-II localized excitons.

A noticeable difference in the behavior of the resonant and nonresonant DQWs concerns the lateral fluctuations of the PL intensity and polarization degree. Both parameters are better reproducible over the surface of the nonresonant DQW. This can be partly explained by the larger width of the GaAs QW in the nonresonant sample and, hence, the weaker effect of the fluctuations of the QW width. One can assume also that the enhanced fluctuations of the PL line polarization [Fig. 5(b)] and shape (Fig. 4) in the resonant structure result partly from the spot-to-spot variation of the atomic configuration of the heterovalent interface, which causes the variation of the dipole moment and, hence, of the CBO value at the heterovalent interface. This effect should be more pronounced in the resonant structure, where even small variation of the CBO leads to a massive type-I to type-II (or vice versa) transformation of excitons, emitting at a certain energy. One should, nevertheless, notice that the shape of the PL line is generally constant over the surface of both structures, except of a few nontypical points of the resonant DQW (see Fig. 4). We believe that these modifications of the spectrum are caused by the especially strong changes of the atomic structure of the heterovalent interface, induced by some unintentional local variations of the growth parameters. The excitonic spectrum of the resonant DQW should be very sensitive to the microscopic variations of the interface structure, because even small change of the interface atomic configuration can result in the variation of CBO of the order of tens and even hundreds of millielectronvolts.[2]

Another difference between the two samples concerns the spin dynamics in an external magnetic field. The observation

of fast spin relaxation in the resonant sample is natural for the DMS structure due to the efficient spin scattering by Mn ions. More intriguing is the rather slow rise of the net spin polarization (8–9 ns) obtained from the fitting procedure for the slow component of the exciton emission band, both in the non-resonant and resonant samples. This value reflects probably the intrinsic spin-relaxation rate of the localized type-II excitons.

V. CONCLUSIONS

We have fabricated an optical-quality GaAs/AlGaAs/ZnSe/ZnCdMnSe DQW with the heterovalent III-V/II-VI interface placed in between of the two QWs as close as at 1–2 nm from the QW boundaries. The excitonic properties of the grown structures depend on the mutual position of the electron levels in the single QWs. In the nonresonant structure with the lowest electron level confined in the nonmagnetic GaAs QW, the recombination dynamics of excitons and the polarization of excitonic spins in an external magnetic field resemble the properties of a conventional GaAs/AlGaAS single-QW of the same width. The main difference is the appearance of a slow-decaying σ^+-polarized contribution to the emission, which was attributed to the recombination of localized type-II excitons. These excitons emerge due to the action of random electric fields generated by the heterovalent interface. Their strong spin polarization results from the effect of giant Zeeman splitting of the electron states, confined in the DMS ZnCdMnSe QW. The behavior of excitons in the resonant structure also resembles the properties expected for supposed isovalent coupled QWs of similar design. The heterovalent interface mainly manifests itself in an additional inhomogeneous broadening of the PL line. Not quite clear at present is the origin of the long spin-relaxation times observed in both resonant and non-resonant samples for the long-living type-II excitons. One possibility is a slow spin relaxation of the fluctuation-localized hole in the GaAs QW, decoupled from the electron of the type-II exciton.

In spite of a special growth procedure, aimed to fabricate the heterovalent interface with zero average dipole moment, fluctuations of the dipole moment on the microscopic scale still seem to be essential. Micro-PL measurements show that these fluctuations occur on the scale less than 1 μm. The fluctuations affect the excitonic properties through the inhomogeneous broadening and generation of the localized type-II excitons. These effects can be disadvantageous for the applications that imply the realization of 2D electron gas with high mobility. On the other hand, the optoelectronic and magnetoelectronic applications relying on the properties of localized carriers are quite possible. The structures of this type can be (In,Ga)As quantum dots coupled to the ZnCdMnSe QW through a heterovalent interface. The spin polarization of electrons in these structures could be flexibly controlled by the application of a relatively weak external magnetic field or an external electric bias.

ACKNOWLEDGMENTS

We acknowledge S. V. Sorokin and I. V. Sedova for the fabrication of samples. This work was supported by the RFBR Grants No. 06-02-16394-a and No. 08-02-91203-jap-a and by the Program of Physical Department of RAS. A.A.T. acknowledges support from the Wenner-Gren Foundation, Sweden, and Russian Science Support Foundation. A.M. acknowledges supports of the Ministry of Education, Science, and Culture, Japan and of the Mitsubishi Foundation. A.G. and J.A.G. acknowledge support of European Project No. MKTD-CT-2005-029671.

[1] R. M. Martin, J. Vac. Sci. Technol. **17**, 978 (1980).
[2] A. Kley and J. Neugebauer, Phys. Rev. B **50**, 8616 (1994).
[3] W. A. Harrison, E. A. Kraut, J. R. Waldrop, and R. W. Grant, Phys. Rev. B **18**, 4402 (1978).
[4] R. Nicolini, L. Vanzetti, G. Mula, G. Bratina, L. Sorba, A. Franciosi, M. Peressi, S. Baroni, R. Resta, A. Baldereschi, J. E. Angelo, and W. W. Gerberich, Phys. Rev. Lett. **72**, 294 (1994).
[5] M. A. Haase, J. Qio, J. M. DePuydt, and H. Cheng, Appl. Phys. Lett. **59**, 1272 (1991).
[6] R. Fiederling, M. Keim, G. Reuscher, W. Ossau, G. Schmidt, A. Waag, and L. W. Molenkamp, Nature (London) **402**, 787 (1999).
[7] S. V. Ivanov, V. A. Kaygorodov, S. V. Sorokin, B. Ya. Meltser, V. A. Solov'ev, Ya. V. Terent'ev, O. G. Lyublinskaya, K. D. Moiseev, E. A. Grebenshchikova, M. P. Mikhailova, A. A. Toropov, Yu. P. Yakovlev, P. S. Kop'ev, and Zh. I. Alferov, Appl. Phys. Lett. **82**, 3782 (2003).
[8] A. A. Toropov, I. V. Sedova, S. V. Sorokin, Ya. V. Terent'ev, E. L. Ivchenko, and S. V. Ivanov, Phys. Rev. B **71**, 195312 (2005).
[9] A. A. Toropov, I. V. Sedova, S. V. Sorokin, Ya. V. Terent'ev, E. L. Ivchenko, D. N. Lykov, S. V. Ivanov, J. P. Bergman, and B. Monemar, Phys. Status Solidi B **243**, 819 (2006).
[10] J. Jasny, J. Sepioł, T. Irngartinger, M. Traber, A. Renn, and U. P. Wild, Rev. Sci. Instrum. **67**, 1425 (1996).
[11] U. Kops, R. G. Ulbrich, M. Burkard, C. Geng, F. Scholz, and M. Schweizer, Phys. Status Solidi A **164**, 459 (1997).
[12] D. Gammon, E. S. Snow, B. V. Shanabrook, D. S. Katzer, and D. Park, Phys. Rev. Lett. **76**, 3005 (1996).
[13] M. Z. Maialle, E. A. de Andrada e Silva, and L. J. Sham, Phys. Rev. B **47**, 15776 (1993).
[14] A. Vinattieri, J. Shah, T. C. Damen, D. S. Kim, L. N. Pfeiffer, M. Z. Maialle, and L. J. Sham, Phys. Rev. B **50**, 10868 (1994).
[15] M. J. Snelling, E. Blackwood, C. J. McDonagh, R. T. Harley, and C. T. B. Foxon, Phys. Rev. B **45**, R3922 (1992).
[16] A. Vinattieri, J. Shah, T. C. Damen, K. W. Goossen, L. N. Pfeiffer, M. Z. Maialle, and L. J. Sham, Appl. Phys. Lett. **63**, 3164 (1993).